6ICEGE 6th International Conference on Earthquake Geotechnical Engineering
1-4 November 2015
Christchurch. New Zealand

Beyond Critical Acceleration Pseudo-Static Analysis

A. Klar[1], N. Lloyd[2], E. Aharonov[3], O. Katz[4]

ABSTRACT

Common geotechnical earthquake engineering design approaches utilize acceleration levels to evaluate slope failure triggering and resulting permanent displacements, using pseudo-static stability analyses together with the Newmark method. These approaches assume a single sliding mechanism and do not take into account the possibility of multiple (increased in size) mechanisms due to higher accelerations than the critical one. This paper presents a "quasi dynamic" analysis framework which allows evaluation of the effect of higher acceleration (beyond the critical one) on the mechanism and the volume of the slide. The approach combines concepts from pseudo-static analysis together with plastic flow, such that the developed mechanisms are restricted from transferring greater stresses than their yield value (and by that preventing factor of safety lower than 1.0). The approach is applied to slopes characterized by ideal elasto-plastic material to demonstrate that in certain conditions an increase in the acceleration level, by itself, may alter the failure mechanism.

Introduction

The pseudo-static analysis is one of the most commonly used techniques for evaluation of the seismic risk of manmade and natural slopes. It may be used as part of factor safety (FS) evaluation under the input of a given acceleration (e.g. Seed, 1979), or for determination of the slope yield acceleration (e.g, Sarma and Bhave, 1974; Sarma 1975; Baker et al. 2006). The latter may be combined with Newmark (1965) analysis for determination of an earthquake induced permanent displacement (e.g. Makadisi and Seed, 1978). The approach assumes that once a mechanism develops, its size and shape remain constant, and the failing slope accelerates with the relative acceleration of $a(t)$-a_y (e.g. Newmark, 1965), where a_y is the yield acceleration (i.e. the acceleration that leads to a factor of safety of 1.0 in a pseudo-static analysis).

Pseudo-static analyses, by their nature, cannot deal with "beyond critical accelerations" (i.e. accelerations higher than those which lead to sliding), as this will only produce a factor of safety smaller than 1.0 and will not reveal information regarding the influence on the mechanism. In fact, sliding mechanisms resulting from pseudo-static analyses with FS<1 are meaningless, as they are associated with artificial, unrealistic, strength properties greater than the real ones

[1]Associate Professor, Department of Structural Engineering and Construction Management, Faculty of Civil and Environmental Engineering, Technion – Israel Institute of Technology, Haifa, Israel, klar@technion.ac.il
[2]Graduate Student, Department of Structural Engineering and Construction Management, Faculty of Civil and Environmental Engineering, Technion – Israel Institute of Technology, Haifa, Israel.
[3]Associate Professor, The Institute of Earth Sciences, The Hebrew University, Givat Ram, Jerusalem 91904, Israel.
[4]Senior researcher, Geological Survey of Israel, 30 Malkhe Israel St., Jerusalem 95501, Israel.

($\phi_{mob}>\phi$, and $c_{mob}>c$). The Newmark (1965) assumption that the slope accelerates by $a(t)$-a_y is correct only if the failure mechanism does not change and the kinematics allows deformation in the direction of the applied acceleration $a(t)$-a_y. This assumption, however, may not always hold. In order to capture the possible impact of greater acceleration on the developed mechanism and displacements, the current paper suggests a "quasi-dynamic" analysis framework which can deal with beyond critical acceleration levels.

The paper is composed of 3 main sections. Firstly the concept of "quasi-dynamic" analysis is presented. Secondly, numerical implementation and an example are provided. Finally, discussion and conclusions are presented.

The "Quasi-Dynamic" Analysis Framework

The Achilles' heel of the pseudo-static analysis is that it cannot limit the mobilized stresses to their yield value. Consequently, analyses with beyond critical accelerations results in mobilized stresses higher than the yield value (hence the FS=τ_y/τ_{mob}<1). In order to examine the slope behavior under accelerations higher than the critical value, one must allow the unbalanced stresses (or loads) to be translated into motion (i.e. acceleration). Let us further discuss this concept using a simple condition of a failure along a predefined, fixed, planar slip surface. Figure 1a shows a given slope subjected to a horizontal acceleration and its free body diagram. Note that due to introduction of kinematics into the current analysis, the dilation angle, ψ, is of importance (unlike conventional pseudo-static limit equilibrium analysis). Figure 1b shows the force polygon associate with the limit state (i.e. FS=1), from which the critical (or yield) acceleration, k_y (=a_y/g), may be defined. Note that the contribution of cohesion is equivalent to an inclined reduced weight at an angle of δ = arccot[$W/(cL\cos\alpha)$-tanα]. Solution of the force polygon shown in Figure 1b, results in a critical acceleration coefficient, k_y, of:

$$k_y = \frac{\cos\alpha}{\cos(\alpha-\delta)}\frac{\sin(\phi+\delta-\alpha)}{\cos(\alpha-\phi)} \quad (1)$$

where, α is the inclination of the slip surface, ϕ is the soil friction angle, and δ angle capturing the effect of cohesion as described earlier. When c = 0 (or δ = 0), k_y degenerates into the well-known solution of a sliding frictional block (with friction ϕ) over an inclined slope of α, k_y = tan(ϕ - α) (e.g. Kramer, 1996). Once acceleration values are higher than k_y, a D'Alembert's force must be introduced into the force polygon in order to consider "static equilibrium" as shown in Figure 1c. Note that the total acceleration body force, kW, is explicitly divided into the yield component, k_yW, and the post yield component, $(k-k_y)W$, to emphasize the contribution of the beyond critical acceleration component. As can be seen, the normal force and frictional forces depend on the acceleration value, and do not remain constant as acceleration increases beyond critical value. The unbalanced force, or the D'Alembert's force, shown as ma (mass times the acceleration), is directed opposite to the movement direction, and is influenced by the dilation angle, ψ. Only when $k = k_y$ the dilation angle does not affect the result, as the force polygon degenerates into that of Figure 1b. An expression for the failed mass acceleration may be obtained from the force polygon (introducing $m=W/g$):

$$\frac{a}{g} = (k - k_y)\frac{\cos(\phi - \alpha)}{\cos(\phi - \psi)} \tag{2}$$

Note that the failed mass accelerates at a value different than $(k\text{-}k_y)g$ (the value suggested by Newmark, 1965), and in fact depends on the dilation angle besides the relative acceleration and sliding directions. For the case of horizontal acceleration input, as discussed here, the mass will accelerate by $(k\text{-}k_y)g$ only if α and ψ are equal to zero.

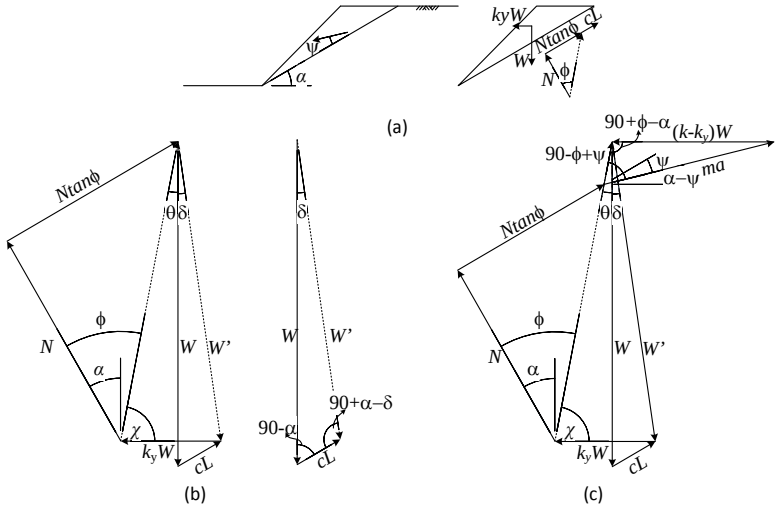

Figure 1. Simplified cases: a. Slope and slip surface; b. Force polygon of limit state of critical acceleration; c. Force polygon for beyond-critical acceleration.

While the above, simplified, case is rather limited, it reveals an interesting point that the unbalanced force (*ma*) is affected by both the volume of the slide and the direction of sliding (associated with the kinematics of yielding). It is therefore postulated that if a "quasi-dynamic" process is considered, in which the acceleration value slowly increases to keep the problem "static" and prevent development of stresses greater than their yield values and stress waves, relations between the unbalanced force (or D'Alembert's force), failure volume, and critical acceleration values could be established. In a sense, any dynamic simulator in which the process of acceleration increase is performed in sufficiently small steps (i.e. slowly) to prevent stress waves while allowing plastic deformation, should allow determination of the quasi-dynamic unbalanced forced (i.e. *ma* in Equation 2). Such analysis may allow insight into the beyond critical acceleration response.

To illustrate the outcome of such a quasi-dynamic process, let us consider a multiple level slope as presented within Figure 2. The domain is subjected to a uniform horizontal acceleration equal to $k \cdot g$. In a "quasi-dynamic" problem, the integrated unbalanced force (IUBF) may be calculated as follows:

$$\text{IUBF} = \int_V \rho\sqrt{\ddot{u}_x^2 + \ddot{u}_y^2}\,dV \tag{3}$$

where ρ is the density, $\ddot{u}_x$ and $\ddot{u}_y$ are the horizontal and vertical acceleration, and V is the volume of the whole domain (including stable areas).

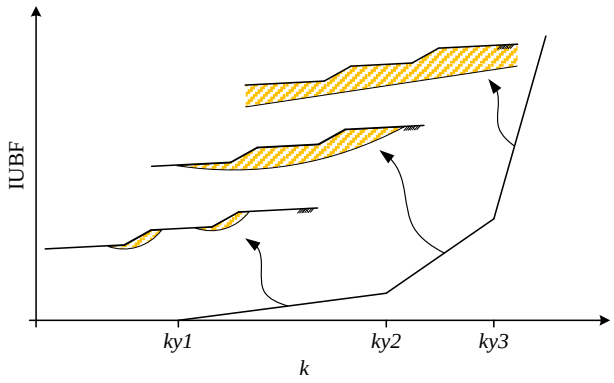

Figure 2. Idealized response of integrated unbalanced force versus applied acceleration.

Figure 2 illustrates how, in principle, the IUBF should be developed with slow increase of accelerations. When k is smaller than the classical critical acceleration, k_{y1}, no failure occurs and the value of IUBF is zero. Once the classical critical acceleration is achieved, sliding begins. As demonstrated by equation 2, for a given mechanism the increase of the IUBF should be proportional to (k-k_y). Consequently, a linear increase of the IUBF with k is expected. Once the sliding mechanism changes, the relationship between IUBF and k should also change, leading to a change in the slope of the IUBF-k line.

Using Equation 2 to establish the unbalanced force, and differentiating it with respect to k, results in:

$$\frac{\partial \mathrm{IUBF}}{\partial k} = V_f \gamma \frac{\cos(\phi - \alpha)}{\cos(\phi - \psi)} \tag{4}$$

where V_f is the volume of the sliding body, and γ is the unit weight of the soil. This expression infers that any change in the IUBF-k slope indicates a change in sliding volume and mechanism. However, in order to establish the volume of the sliding mass, one must estimate the value of α in addition to the IUBF-k slope, assumed to be the average slip surface inclination (as in Taylor (1937) friction-circle method). It is suggested that α be determined as $\theta_{\mathrm{IUBF}}+\psi$, where θ_{IUBF} is the direction of the global unbalanced force:

$$\theta_{\mathrm{IUBF}} = \arctan\left(\int_V \ddot{u}_y dV \Big/ \int_V \ddot{u}_x dV \right) \tag{5}$$

The following section details how the “quasi-dynamic” process may be achieved using finite difference analysis.

Numerical Implementation and Example

The numerical implementation of the described “quasi-dynamic” process was achieved using the equilibrium solver of the finite difference code *FLAC* (Itasca, 2013). *FLAC* solves the equations of motion together with artificial mass and high damping, applied only when changes in velocity

direction occur (to damp dynamic waves while allowing continuous plastic flow). Conventionally, equilibrium is declared, within *FLAC*, when the maximum unbalanced force diminishes to a small portion of the applied gravitational force. This way static and plastic flow problem can be solved using the equations of motions. The current implementation utilizes a very similar process, in which, except for gravitational loads, the complete domain is subjected to a horizontal body force of $\rho \cdot k \cdot g$. The value of the integrated unbalanced force (Equation 3) is continuously monitored. A solution is declared once the IUBF reaches a constant value over time (steps). This infers that all dynamic waves have been dissipated and the domain is either stable (if the IUBF is nearly zero) or reached a state of constant acceleration (the "quasi-dynamic" condition). The process begins with a low value of k, which slowly increases in small increments. In each increment the development of a constant IUBF is awaited before proceeding to the next increment. The evaluation process is performed within a framework of small strains without any coordinates update (such that the slope remains in place as a boundary value problem).

Figure 3 shows the finite difference model of an infinite multi-leveled natural slope. Periodic boundaries were used, together with a simulation process of top-down erosion to generate also periodic initial stress condition. The average (infinite slope) inclination is 6.3 degree while the maximum is 30 degree. The maximal height difference between toe and crest is 10 meter. Figure 4 shows the results of the IUBF versus the applied acceleration coefficient, k, for a case in which the $\rho = 1.8 \cdot 10^3 \text{kg/m}^3$, $\phi = 30$ degree, $c = 5$ kPa and $\psi = 0$ degree and the analysis is performed with an elastic perfectly plastic constitutive model answering a yield function of Mohr-Coulomb. The elastic parameters were shear modulus of 30 MPa and bulk modulus of 65 MPa.

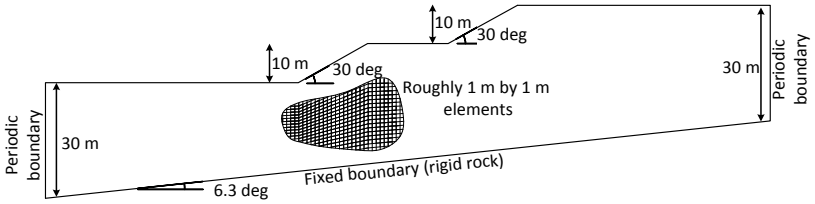

Figure 3. Boundary value problem and finite difference grid.

As can be seen, first yielding occurs at horizontal acceleration of roughly 0.2g, and is associated with individual local slope failure (as illustrated in Figures 2 and 5a). At acceleration of approximately 0.33g the mechanism changes to a global two-slope failure (as illustrated in Figures 2 and 5b). Once the acceleration reaches a value of 0.38g a global, infinite, slope failure occurs (as illustrated in Figures 2 and 5c). Note that conventional infinite slope stability evaluation based on Mohr-Coulomb yield failure ($\tau_f = \sigma \cdot \tan\phi + c$) results in:

$$k_y(z) = \frac{c\cos\phi}{z\gamma\cos\alpha\cos(\phi-\alpha)} + \tan(\phi-\alpha) \tag{6}$$

where z is the depth for which the infinite planar slip surface is located. For the current case, in which $z = 30$ meter, this expression yields k_y of 0.44, which is greater than the obtained value from the numerical simulation (0.38). The reason is shear band formation and post-peak failure

(e.g. Vermeer, 1990). That is, even in elastic perfectly plastic constitutive model, strain softening may occur when the dilation angle is smaller than the internal friction angle. As shown by Vermeer (1990), for plane strain simple shear condition the ratio between the shear stress and normal stress at post-peak residual yielding is:

$$\frac{\tau_{f\,(residual)}}{\sigma} = \tan\phi^* \equiv \frac{\cos\psi \sin\phi}{1-\sin\psi \sin\phi} \tag{7}$$

Introducing ϕ^* into Equation 5 instead of ϕ, results in a k_y of 0.378 - a practically identical value to that obtained from the numerical results. When the analysis is performed with $\psi = \phi$ (and consequently $\phi^* = \phi$) the infinite slope failure occurs at the conventional value of Equation 5. Note that this phenomenon of strain softening along shear bands is not limited to this specific problem. However, the fact that in the current problem shear strains are accumulated leads to this condition.

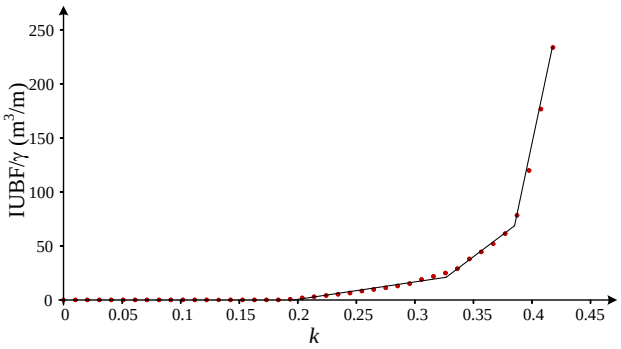

Figure 4. Simulation results for the slope shown in Figure 3 with $\rho = 1.8 \cdot 10^3$kg/m^3, $\phi = 30$ degree, $c = 5$ kPa and $\psi = 0$ degree.

Table 1 shows a comparison between the slide volumes evaluated by the slope of the curve in Figure 4 together with Equation 4 and $\alpha = \theta_{IUBF} + \psi$ against the volume of sliding based on numerical measurements of sliding elements in *FLAC*. That is, the value of V_f denoted by *FLAC* in the table was obtained by summing the area of all zones having a velocity greater than 0.1 the maximal velocity. While this may not be the most accurate method, it still provides a rough estimate of the sliding areas, since difference in velocity between stable and failing zone is abrupt (most of the velocity change occurs over a thin shear band – roughly one element). Mechanism 1 2 and 3 are associated with the 3 slopes observed in Figure 4. Figure 5 shows the associated volume in *FLAC* based on the 0.1 maximum velocity criterion. Note that since α was defined based on the direction of the IUBF, for the infinite slope it results in a slightly greater value than the slope itself (= 6.3 degree). As can be seen from the comparison, the procedure suggested in this paper appears to give a reasonable and consistent evaluation of the volume of slides, based only on the value of the unbalanced force and its direction. It should be noted that the force polygon presented in Figure 1c and the corresponding equation (4) (together with $\alpha = \theta_{IUBF} + \psi$) for sliding volume determination are associated with an ideal case of a single slide over a planar surface. It is therefore most suitable for the first local slides, and its use for volume determination of multiple slides can only be considered a rough approximation. This is because the kinematics of lower slip surfaces will affect the direction of the motion of upper slip surfaces and their corresponding unbalanced force. In fact, once Mechanism 2 develops, the

lower and upper 10 m slopes (previously identical) behave differently (considering a rotational global behavior of the lower slip-surface). This effect can also be seen in the comparison table. The agreement for Mechanism 1 appears to be very good (0.1% difference), since at this point only local slides occur. Once the mechanism is extended to include a deeper slip surface, the agreement worsens (5% difference). When global, infinite, mechanism develops, the agreement becomes good again. This is because the overall contribution of the large slide overshadows the effect of the small slides.

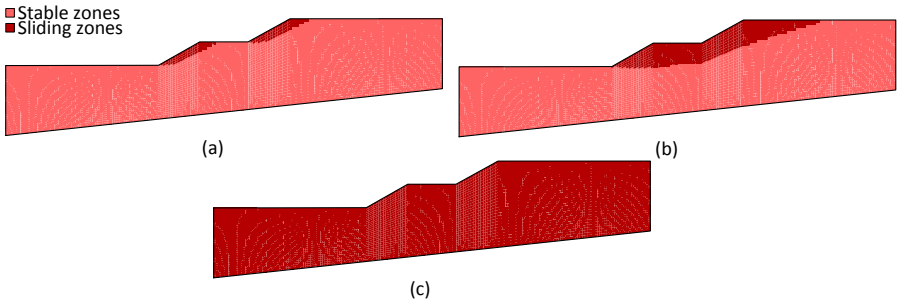

Figure 5. Sliding volumes based on 0.1 maximum velocity criterion. Mechanisms developed at accelerations (a) k=0.25 (b) k=0.37 (c) k=0.42.

Table 1. Comparison of sliding mass volume.

		Mechanism 1	**Mechanism 2**	**Mechanism 3**
α [deg] = $\theta_{IUBF} + \psi$		23.3	15.6	6.7
$V_f [m^3/m]$	*FLAC*	153.4	828.3	5225
	Equation 4	153.2	871.0	5263.9
Difference [%]		0.1	4.9	0.7

Conclusions

Geotechnical earthquake engineering design approaches frequently utilize the acceleration levels to evaluate slope failure triggering and resulting permanent displacements, using pseudo-static stability analyses together with Newmark method. These approaches involve an implicit assumption of a single sliding mechanism of a constant volume, and do not take into account the possibility of multiple, increased in size, mechanisms due to higher acceleration than the critical one. That is, evaluation of the slope under higher acceleration than the critical one only results in a factor of safety smaller than 1.0 and cannot capture the possible impact of greater accelerations on the developed mechanism and displacements.

The paper presents an analysis framework which allows evaluation of the effect of higher accelerations (beyond the critical one) on the mechanism and the volume of the slide. The approach combines concepts from pseudo-static analysis together with plastic flow, such that the developed mechanisms are restricted from transferring greater stresses than their yield values

(and by that preventing factor of safety lower than 1.0). The approach may be said to be “quasi dynamic” in which the failing mass continues to accelerate under the unbalanced forces (beyond the critical one), while the remaining stable body is static, until an additional, new, mechanism develops. In the paper, the approach is applied to slopes characterized by ideal elasto-plastic material to demonstrate that in certain conditions an increase in the acceleration level, by itself, may alter the slope failure mechanism. It is demonstrated that changes in failure mechanism occur at distinct acceleration levels (the first of which is the classical pseudo-static value), and the volume of the sliding mass correlates with the integrated unbalanced force.

The effect of mechanism alteration due to increase in acceleration may be more relevant to natural slopes, in which individual local modes of failure may unite into a larger global failure mode, but not necessarily to manmade embankments in which a change of mechanism requires drastically high accelerations.

The fact that distinct acceleration levels separate between small and large sliding volumes may potentially be used for geological and geographical statistical evaluation of seismic history based on landslides scars, such that an area characterized by a diversity of landslide volumes may be said to be exposed to greater accelerations (leading to the second or third mechanism) while an area with only local failure to much smaller accelerations.

Note that landslide volumes may well depend on other parameters except for acceleration levels alone. For example if the material is sensitive, with significant strain softening, earthquake magnitude may govern the behavior (as the strain accumulation and loading cycles increase with magnitude). Such effects may potentially be incorporated into the suggested framework through equivalent cyclic based degradation parameters. This, however, requires further study.

Acknowledgments

This research was funded by the Israeli Ministry of Science, Technology and Space (grant number 3-9145).

References

Baker, R., Shukha, R., Operstein, V., Frydman, S. Stability charts for pseudo-static slope stability analysis. *Soil Dynamics and Earthquake Engineering*, 2006, **26**, (9): 813–823.

Itasca. *FLAC ver. 7 – User manual. Itasca* Consulting Group. Minneapolis. 2013

Kramer, S.L. *Geotechnical Earthquake Engineering*. Prentice Hall, 1996.

Makdisi, F., Seed, H. Simplified procedure for estimating dam and embankment earthquake induced deformations. *J. Geotech. Engrg. Div*. 1978, **104**,(7): 849–867.

Newmark, N. M. Effects of earthquakes on dams and embankments. *Geotechnique* 1965, **15**,(2): 139–160.

Sarma S. K. Seismic stability of earth dams and embankments. *Geotechnique* 1975, **25**, (4):743–61.

Sarma SK, Bhave MV. Critical acceleration versus static factor of safety in stability analysis of earth dams and embankments. *Geotechnique* 1974, **24**,(4):661–5.

Seed, H. B. Considerations in the earthquake-resistant design of earth and rockfill dams. *Geotechnique* 1979, **29,** (3): 215–263.

Taylor, D. W. Stability of earth slopes. *J. Boston Soc. Civil Eng*. 1937, XXIV(3): 337–386.

Vermeer, P. The orientation of shear bands in biaxial tests. *Geotechnique* 1990, **40**, (2): 223–236.